Review Article for Residents

Dynamic corneal deformation response and integrated corneal tomography

Marcella Q Salomão[1,2,3], Ana Luisa Hofling-Lima[1], Fernando Faria-Correia[2,4,5,6], Bernardo Teixeira Lopes[1,2,3], Sandra Rodrigues-Barros[1,2,7], Cynthia J Roberts[8], Renato Ambrósio Jr.[1,2,3]

Measuring corneal biomechanical properties is still challenging. There are several clinical applications for biomechanical measurements, including the detection of mild or early forms of ectatic corneal diseases. This article reviews clinical applications for biomechanical measurements provided by the Corvis ST dynamic non contact tonometer

Key words: Corneal biomechanics, corneal tomography, ectasia, keratoconus

Access this article online

Website: www.ijo.in

DOI: 10.4103/ijo.IJO_831_17

Quick Response Code:

One of the major challenges of modern ophthalmology is to accurately measure corneal biomechanical properties. *Ex vivo* laboratory studies[1] and mathematical corneal models[2,3] paved the way to *in vivo* biomechanical assessment, which was first available in 2005 with the ocular response analyzer (ORA), developed by David Luce.[4] The ORA is a modified noncontact tonometer (NCT) designed to provide a more accurate measurement of intraocular pressure than Goldmann tonometry by compensating for corneal biomechanics. The ORA provides estimates of corneal hysteresis and corneal resistance factor following the applanation induced by an air jet.[4]

Potential clinical applications of assessing corneal biomechanics include greater understanding of intraocular pressure and corneal treatments such as elective laser vision refractive surgery, corneal crosslinking (CXL), and corneal incisions, as these procedures might induce changes in biomechanical response.[5] In addition, it is presumed that in keratoconus and other ectatic corneal diseases, the changes in curvature, elevation, and pachymetry, which in fact, remain the focus of clinical investigation in our daily practice, are most likely secondary to a focal weakening that initiates a biomechanical decompensation.[6,7] Thus, early identification and recognition of an eventual biomechanical flaw, beyond corneal shape analysis, might possibly enhance our sensitivity to detect milder forms of ectatic diseases.

The identification of milder or sub-clinical forms of ectatic corneal diseases became crucial following the latest developments in refractive surgery. Indeed, these cases are typically at very high risk for developing iatrogenic progressive ectasia (keratectasia) after laser vision correction (LVC).[8-10] Nevertheless, the current concept for screening ectasia risk goes beyond the detection of mild cases of ectasia,[9] toward the characterization of biomechanical susceptibility if an additional structural impact is induced by the procedure. In addition, the need to increase sensitivity to detect early stages of the disease and also monitor its progression has also been boosted by the advent of new therapeutic alternatives for ectatic diseases, such as corneal CXL and intrastromal corneal rings segments.[11,12]

Certainly, the advent of front surface corneal topography improved our ability to detect ectasia in stages before the development of symptoms such as loss of visual acuity, or the appearance of clinical slit lamp signs.[13,14] Corneal topography subsequently evolved to three-dimensional (3D) tomography, with front and back surfaces characterization, along with a thickness map.[15] Studies have demonstrated the ability of this technology to detect mild, "forme fruste" or subclinical keratoconus in eyes with "innocent", relatively normal topographic map from patients with contra-lateral clinical

[1]Department for Ophthalmology, The Federal University of Sao Paulo, Sao Paulo, [3]Department of Ophthalmology, Instituto De Olhos Renato Ambrósio and VisareRIO, Rio de Janeiro, Brazil, [4]Department of Cornea and Refractive, Hospital De Braga, [6]Department of Ophthalmology, School of Health Sciences, University of Minho, Braga, [5]Department of Cornea and Refractive, Institute CUF Porto, Porto, [7]Departamento De Oftalmologia, Hospital Garcia de Orta, Almada, Portugal, [8]Departments of Ophthalmology and Visual Science and Biomedical Engineering, The Ohio State University, Columbus, Ohio, USA, [2]Rio de Janeiro Corneal Tomography and Biomechanics Study Group

Correspondence to: Dr. Renato Ambrósio Jr., Rua Conde de Bonfim, 211/712, Rio de Janeiro, Brazil. E-mail: dr.renatoambrosio@gmail.com

Manuscript received: 21.09.17; Revision accepted: 25.10.17

Cite this article as: Salomão MQ, Hofling-Lima AL, Faria-Correia F, Lopes BT, Rodrigues-Barros S, Roberts CJ, *et al*. Dynamic corneal deformation response and integrated corneal tomography. Indian J Ophthalmol 2018;66:373-82.

ectasia.[16,17] Similarly, a tomographic approach has augmented the ability to detect ectasia risk or susceptibility in retrospective studies of patients who developed keratectasia after LASIK despite normal pre-operative topographic and pachymetric analysis.[18,19] Finally, the combination of biomechanical and tomographical data was found to be especially helpful to enhance the overall diagnostic accuracy of mild forms of ectatic corneal disease in additional studies.[18,20]

In this article, we review the clinical applications for biomechanical assessments provided by the Corvis ST, a NCT which utilizes an ultra-high-speed (UHS) Scheimpflug camera to monitor dynamic corneal deformation along with the integration with Pentacam corneal and anterior segment tomography.

The Corvis ST Dynamic Scheimpflug Analyzer

Introduced at the AAO meeting in 2010, the Corvis ST (Oculus, Wetzlar, Germany), is a NCT system with a collimated air pulse with consistent pressure profile, that acquires 4300 frames/s using an UHS Scheimpflug camera with ultraviolet-free 455 nm blue light, covering 8.5 mm horizontally of a single slit to allow evaluation of corneal deformation.[21-23] During the measurement, an air puff deforms the cornea inward to the first applanation and then into concave shape, to the point that the highest concavity (HC) is achieved [Fig. 1]. Afterward, the cornea recovers in the outward direction and undergoes a second applanation before returning to its natural position. Timing and corresponding pressures are monitored throughout the measurement. Once the measurement is performed, the device provides a set of corneal deformation parameters, based on the dynamic inspection of the corneal response, including analysis of those parameters that are extracted at the HC point [Table 1].[22-24] The Corvis ST uses a calibration factor to calculate the intraocular pressure (IOP) value based on the pressure that at the time of the first applanation.[22] The biomechanical-compensated IOP, available in the Vinciguerra Screening Report [Fig. 2] is then corrected through a finite element method, using deformation data beyond central corneal thickness and age, including the deformation response.[25-27]

Ramos and collaborators summarized and demonstrated the relevance of dynamic Scheimpflug imaging evaluation for several clinical conditions in a film, available at https://www.youtube.com/watch?v=VQj1pVexW8c. Other investigators also described additional clinical applications of dynamic 3D evaluation in daily practice,[28,29] and acceptable repeatability for the key parameters has also been reported.[22,30,31] The role of dynamic corneal deformation response (DCR) analysis for an accurate intra-ocular pressure measurement was also illustrated in a study from Faria-Correia and collaborators.[28] The authors reported tomographic and biomechanical findings in a case of ocular hypertension in pressure-induced stromal keratopathy, which had been misdiagnosed as diffuse lamellar keratitis after LASIK due to dramatic underestimation of IOP using Goldmann Applanation tonometry.[28]

The ability to enhance accuracy to detect ectatic corneal diseases has been expected since the Corvis prototype was tested,[18] but in fact, the first set of proposed parameters

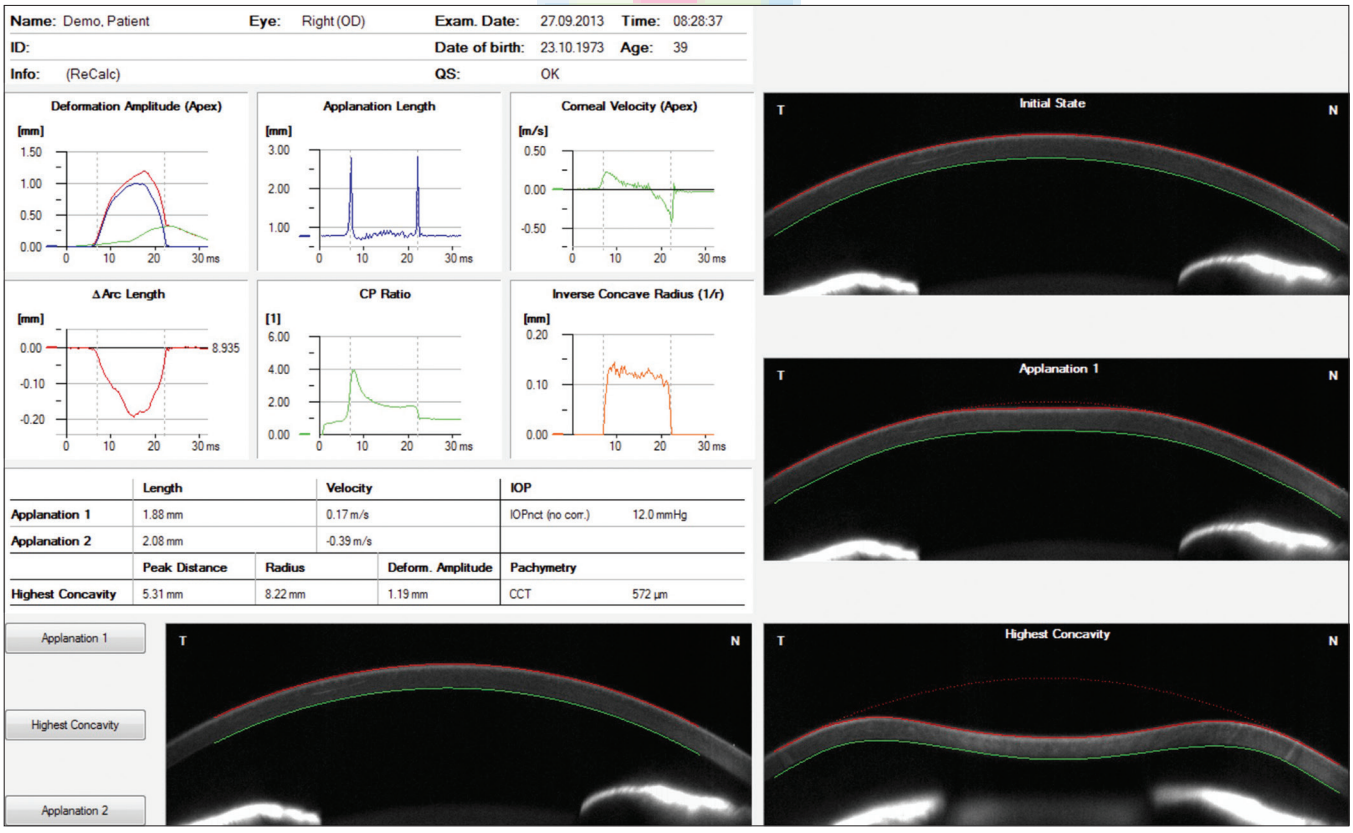

Figure 1: Corvis ST overview display

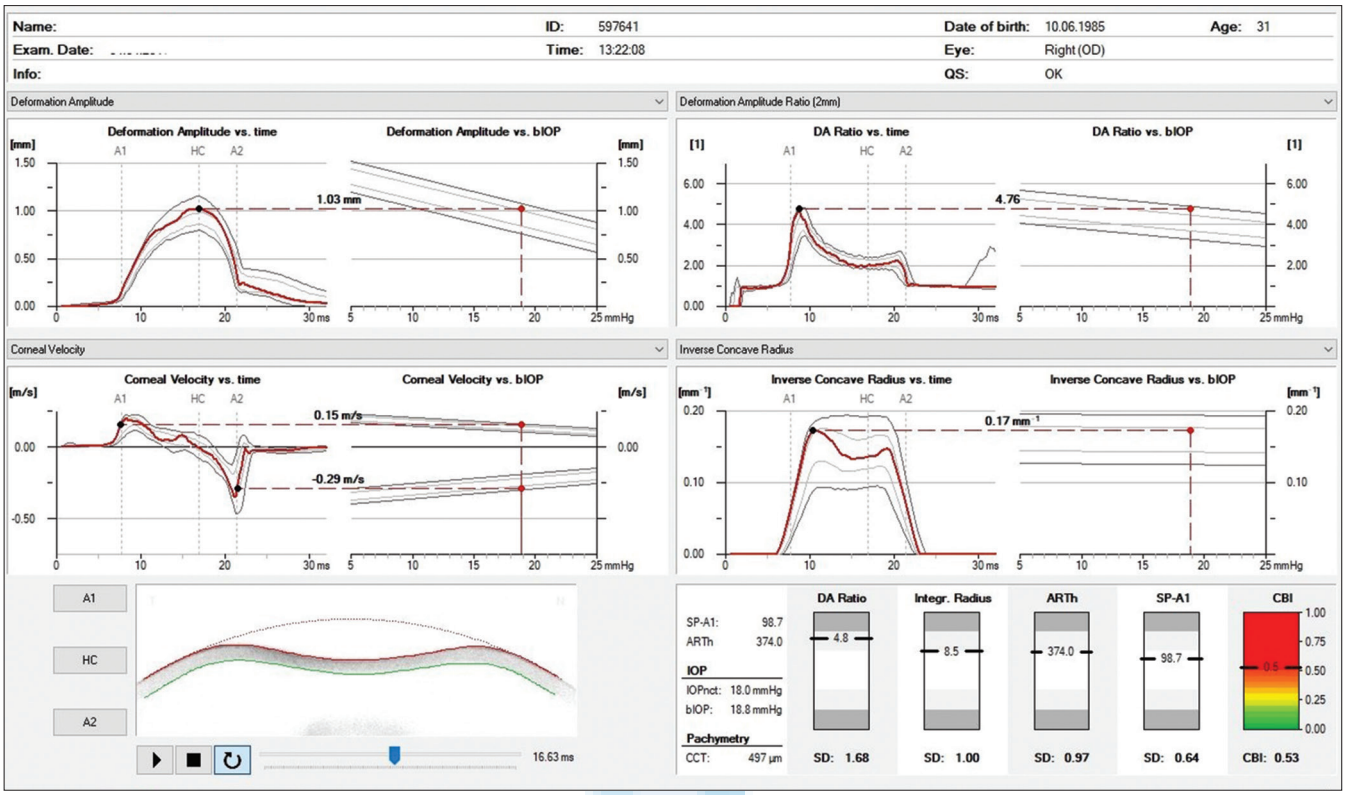

Figure 2: Corvis ST corneal biomechanical index display

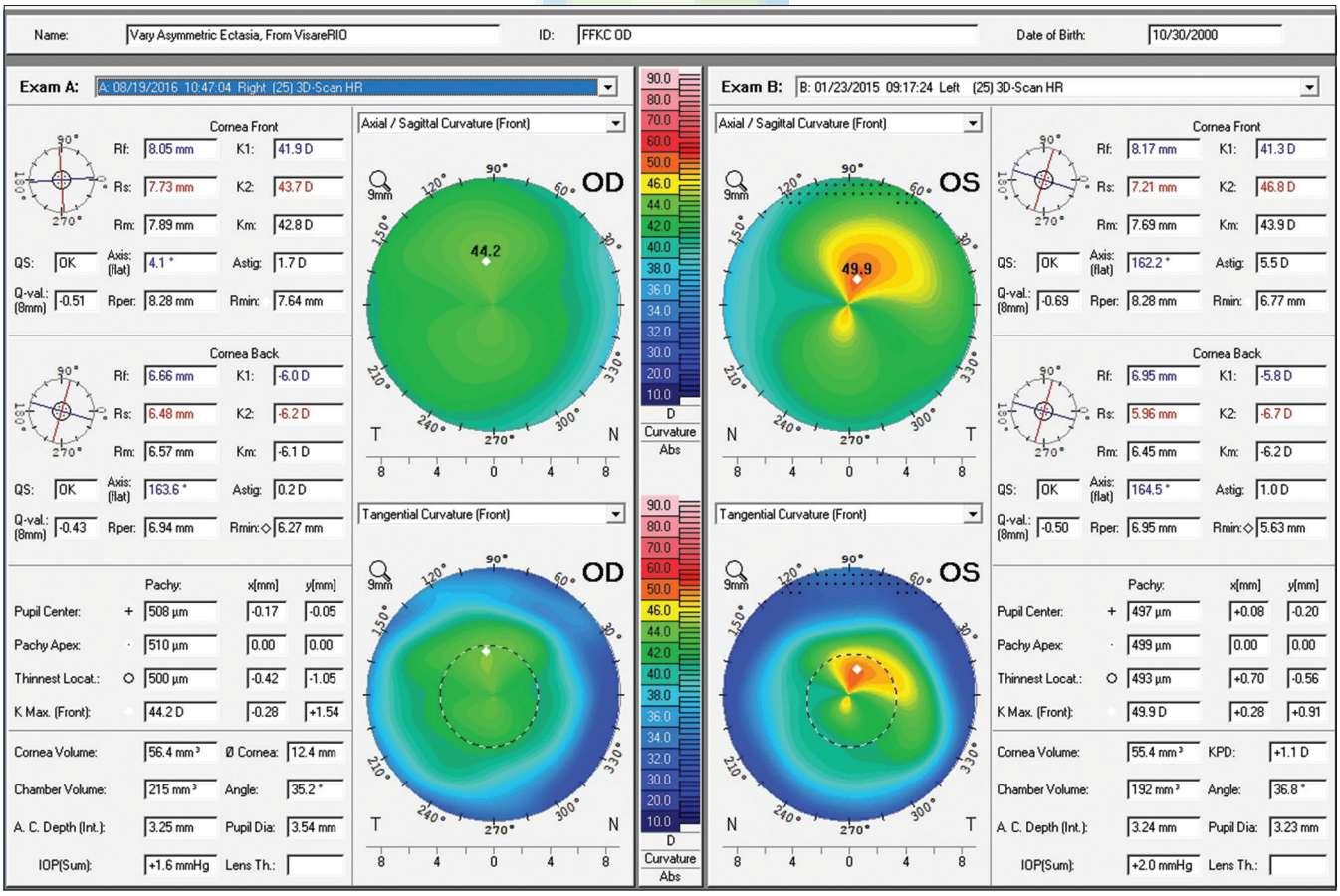

Figure 3: Axial and tangential curvature maps of the front corneal surface from both eyes, obtained with the Pentacam HR corneal tomography (Oculus Optikgeräte GmbH, Wetzlar, Germany). Very mild asymmetry is observed in OD and advanced KC in OS

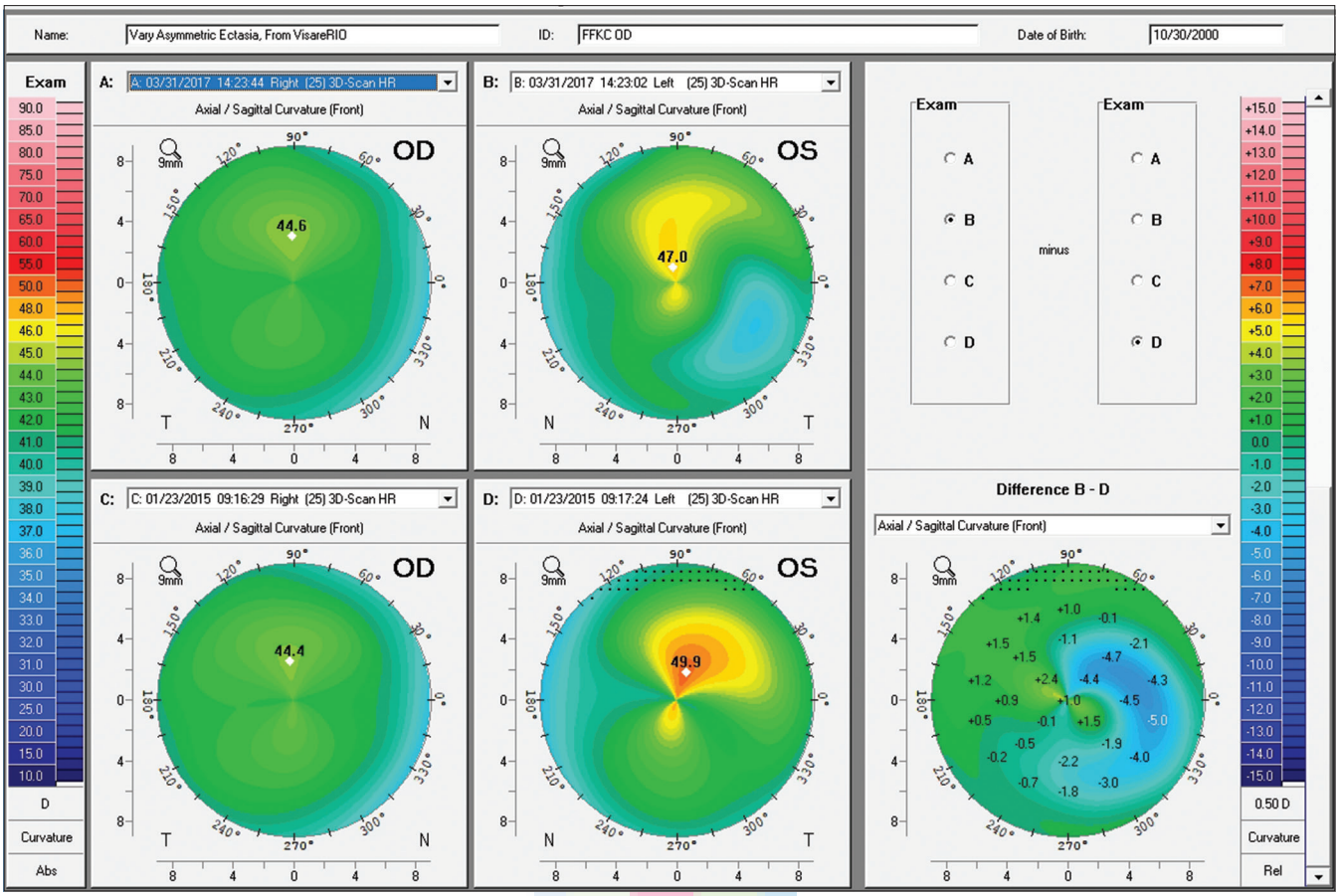

Figure 4: Anterior surface corneal topography from OD at the first visit in 2015 (C) and with 2 years of follow up in 2017 (A). Anterior surface corneal topography from OS in pre (D) and post operative (B) periods

Table 1: CORVIS ST - PARAMETERS

1st Applanation	Moment at the first applanation of the cornea during the air puff (in miliseconds). In parenthesis is the length of the applanation at this moment (in milimeters)
Highest Concavity	Moment that the cornea assumes its maximum concavity during the air puff (in miliseconds). In parenthesis is the length of the distance between the two peaks of the cornea at this moment (in milimeters)
2nd Applanation	Moment at the second applanation of the cornea during the air puff (in miliseconds). In parenthesis is the lenght of the applanation at this moment (in milimeters)
Maximum Deformation	Measurement (in milimeters) of the maximum cornea deformation during the air puff
Wing Distance	Length of the distance between the two peaks of the cornea at this moment (in milimeters)
Maximum Velocity (in)	Maximum velocity during the ingoing phase (in meters per secons [m/s])
Maximum Velocity (out)	Maximum velocity during the outgoing phase (in meters per secons [m/s])
Curvature Radius Normal	Radius of curvature of the cornea in its natural state (in milimeters)
Curvature Radius HC	Radius of curvature of the cornea at the time of maximum concavity during the air puff (in milimeters)
Cornea Thickness	Measurement of the corneal thickness (in milimeters)
IOP	Measurement of the intraocular pressure (in milimeters of Mercury [mmHg])
DAratio 2 mm	Ratio between vertical displacement at apex and at 2 mm
Inverse concave Radius	Inverse of the Radius of curvature during concave phase of the deformation
Integrated Radius	Area under the inverse concave Radius vs. time curve
SP-A1	Parameter reflecting bending stiffness of the cornea as defined by force/replacement
bIOP	Biomechanical corrected IOP
CBI	Corvis Biomechanical Index: overall biomechanical index for kc detection
TBI	Tomographic Biomechanical Index: combines tomographic and biomechanical data for enhanced ectasia detection

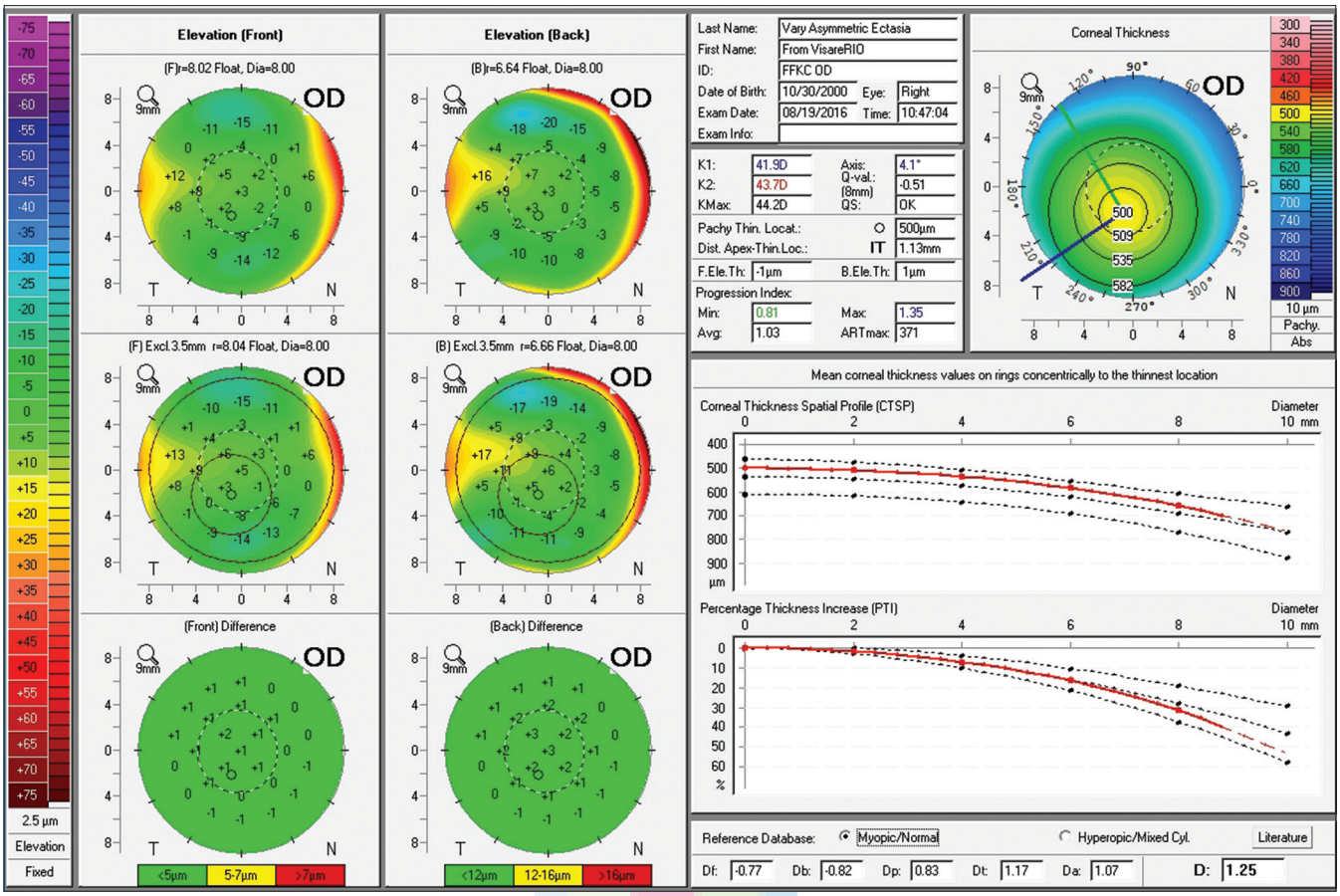

Figure 5: Belin-Ambrósio Enhanced Ectasia Display from the Pentacam of OD. Note ARTmax value of 371 and Belin/Ambrósio Deviation of 1.25

derived from the Corvis ST was found to have a relatively poor ability to discriminate between normal and keratoconic eyes, using the original set of deformation parameters available on the device.[32,33] A retrospective study performed with the Corvis prototype raised the hypothesis that normal eyes (group N) and eyes with topographic patterns suspicious of keratoconus but documented as stable for at least 1 year and with normal tomography (group Stable-KCS), would have different deformation responses compared to ectatic corneas, including keratoconus eyes (KC group) and eyes with normal topographic patterns from cases with very asymmetric keratoconus (group FFKC). Although statistically significant distributions were found for all studied parameters between N and KC groups, there was a substantial overlap and the area under the ROC curve of the best parameter was of 0.852.[34] Thus, to maximize the separation between N and KC groups through a combination of parameters, a linear regression analysis model was calculated by the BrAIN (Brazilian Study Group of Artificial Intelligence and Corneal Analysis) group, finding the Corvis Prototype-Factor 1 (CPF-1), which enhanced the AUC to 0.945. Complementary statistical analysis found no differences on CPF-1 for the FFKC and KC groups and for the N and KCS groups, but there were significant differences for N versus FFKC, N versus KC, stable-KCS versus FFKC and stable-KCS versus KC.[34] This study demonstrated the potential for the data derived from this instrument to effectively distinguish normal and ectatic corneas, even in cases with mild topographic changes.

Several other studies focusing on the diagnosis of keratoconus employing the Corvis ST have been released in the literature in recent years.[21,32,35] Ali and collaborators compared dynamic Scheimpflug measurements between normal and keratoconic eyes and found that despite not having a good discriminative ability alone, the deformation amplitude was useful in diagnosis and monitoring of the disease.[32] Another study comparing normal and keratoconic eyes found the majority of the biomechanical variables derived from the Corvis ST (deformation amplitude, maximum corneal inward velocity, maximum corneal outward velocity, and maximum deformation area) to be significantly different between the groups.[21]

In 2014, a multicenter international group for the study and improvement of the Corvis ST parameters was formed. The main focus of this task force was to maximize accuracy in detecting ectatic corneal diseases, at first exploring corneal deformation data but posteriorly integrating corneal tomography data from Pentacam. Vinciguerra and coworkers combined the DCR data and the horizontal thickness profile[36] for introducing the Corvis (or corneal) biomechanical index (CBI),[37] a parameter developed based on logistic regression analysis which combined deformation response parameters with corneal thickness profile [Fig. 2]. This international collaborative study involved one eye randomly selected from 180 keratoconic patients and from 478 normals, and results of the training database showed that 98.2% of the cases were correctly classified, with 100%

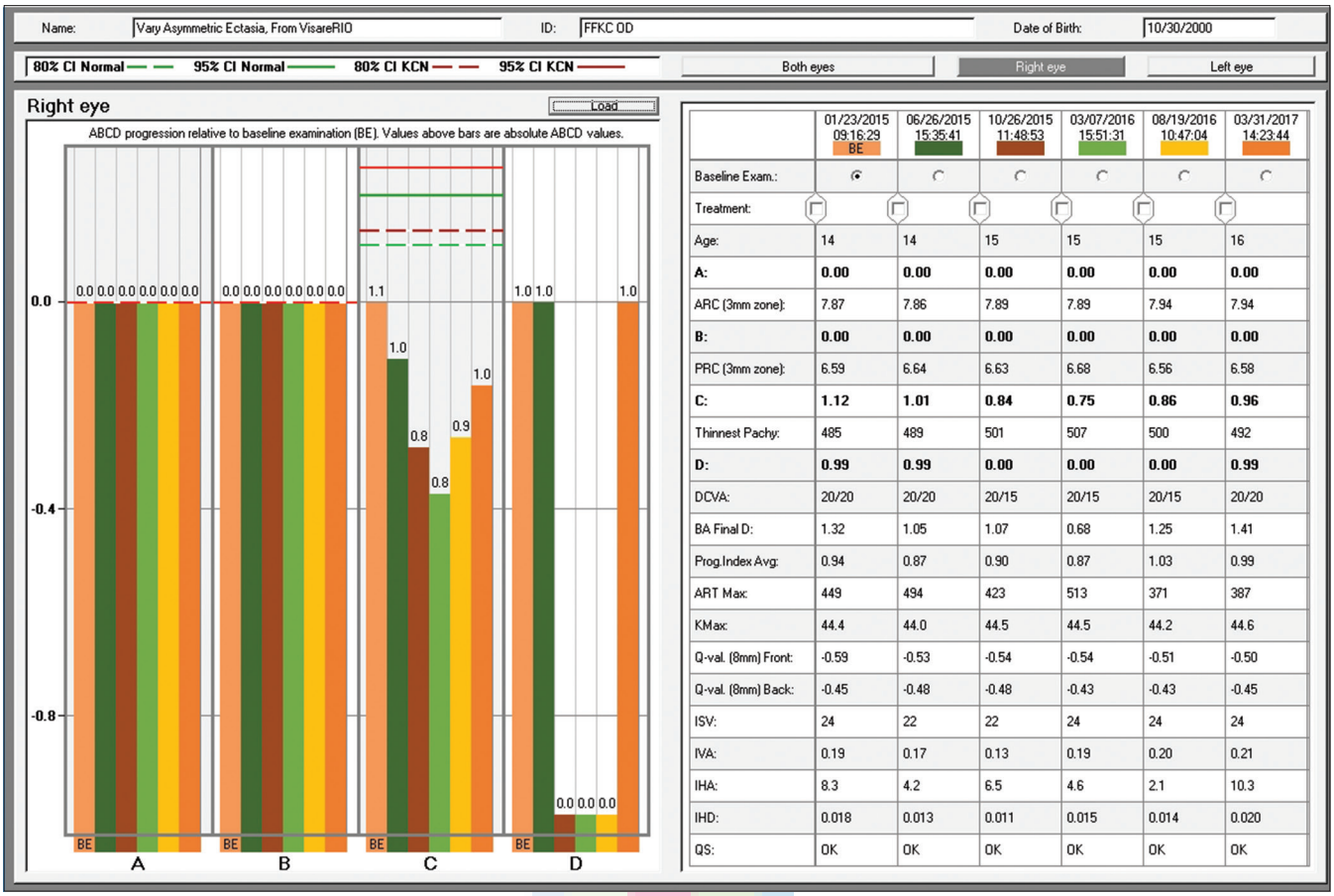

Figur 6: D-The Belin ABCD keratoconus staging

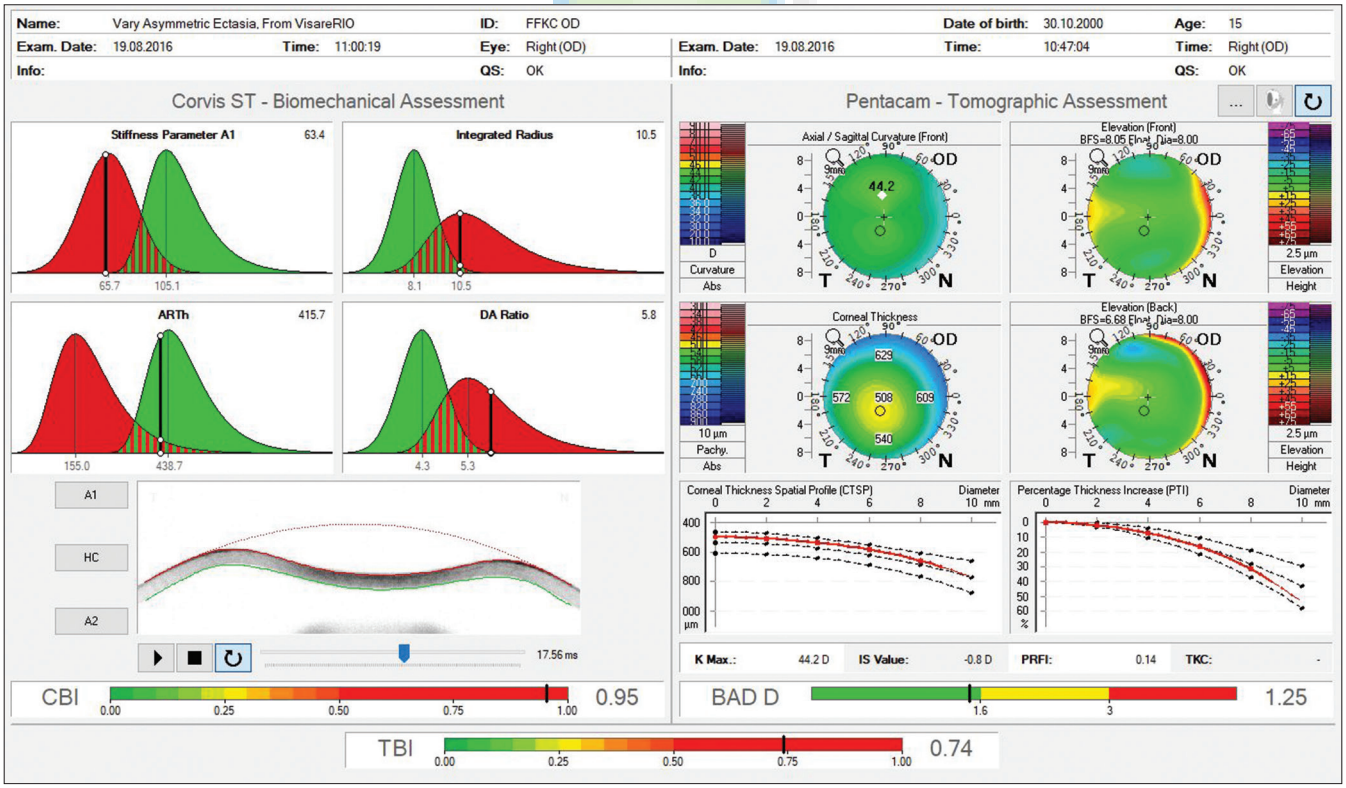

Figure 7: Ambrósio, Robers and Vinciguerra tomographic/biomechanical index display. Observe an abnormal corneal biomechanical index value of 0.95 and abnormal tomographic/biomechanical index value of 0.74

specificity and 94.1% sensitivity using a cut-off of 0.5. The area under the curve was 0.983. Subsequently, in the validation dataset, the same cut-off point correctly classified 98.8% of the cases, with 98.4% specificity and 100% sensitivity.[37] The same group presented a case series of patients with subclinical ectasia with normal topometric (anterior curvature) and also normal tomographic findings in one eye, including the Belin/Ambrósio Enhanced Ectasia total deviation index (BAD-D) from the Pentacam less than 1.6 who showed abnormalities detected by the CBI.[38]

Ambrósio and coworkers developed a combined parameter based on tomography data from the Pentacam (OCULUS Optikgeräte GmbH; Wetzlar, Germany) and biomechanical assessment from the Corvis ST. This multicenter study introduced a novel index for enhanced ectasia detection, the tomographic/biomechanical index (TBI) Figs. 3e and 4c.[10] The study involved one eye randomly selected from 480 patients with normal corneas and from 204 keratoconus patients (Groups I and II, respectively), along with 72 nonoperated ectatic eyes (Group III), from 94 patients with very asymmetric ectasia (VAE), whose fellow eyes (Group IV) presented with normal topography. Results showed that using a cut-off of 0.79, TBI provided 100% sensitivity for detecting clinical ectasia (groups II and III) with 100% specificity, as well. The AUROC for detecting ectasia (Groups II, III and IV) of TBI was 0.996, being statistically higher than tomographic parameters alone and CBI alone. In Group IV, an optimized TBI cut-off value of 0.29 provided 90.4% sensitivity and 96% specificity; and the area under the ROC curve was 0.985. This study demonstrated the added benefit of corneal deformation response data to the geometric analysis to provide improved accuracy for the diagnosis of very mild forms of ectasia.

The CBI and the TBI were developed to detect/screen for ectasia risk before LVC. Considered the LVC procedure does thin and weaken the cornea, the current algorithms would likely be positive after surgery even in stable cases. This may be important to clarify that a novel index is developed to detect post-LASIK ectasia.

External validation studies including one eye from 100 patients with mild keratoconus with central K less than 48D from India (Padmanabhan), and 24 patients with VAE from Iran (Momeni-Moghaddam) have also been conducted. A normal control group with one eye from 100 normal cases from India and from 34 normal patients from Iran were also included. The cutoff value of 0.79, which had 100% sensitivity for frank ectasia with 100% specificity in the original study, had 99% sensitivity and 100% specificity in the India population and 100% sensitivity for the ectatic eyes with 100% specificity in the cases from Iran. Considering the eyes with normal topography from the 24 VAE cases from Iran, the optimized TBI cutoff of 0.27, which had 90.4% sensitivity and 96% specificity in the original study, provided 91.6% sensitivity with 97% specificity. Such data validate the hypothesis that the TBI may potentially epitomize the inherent ectasia susceptibility of the cornea.

The clinical examples illustrate the benefits of such diagnostic approach to enhance both sensitivity and specificity for detecting ectasia which plays a fundamental role when screening laser refractive surgery candidates.

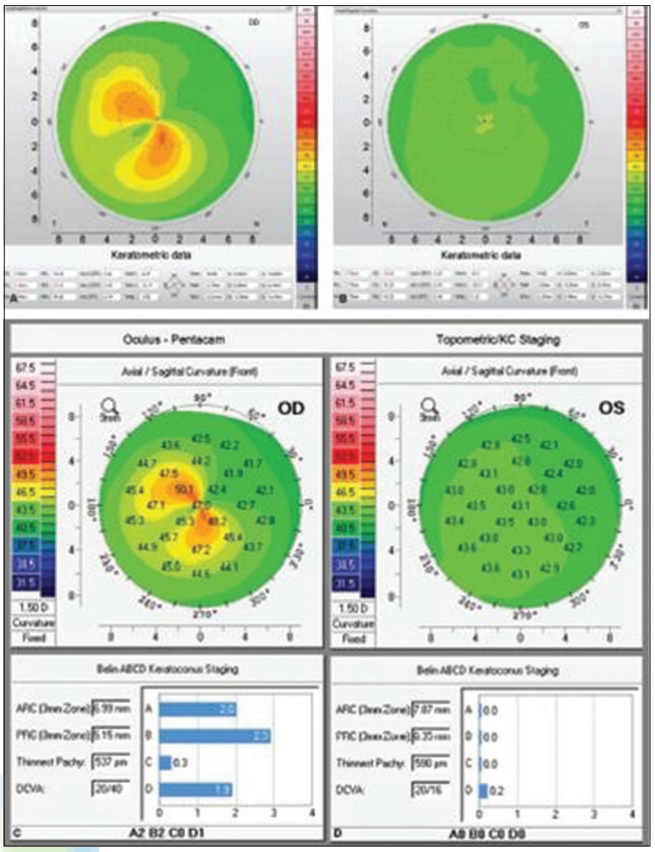

Figure 8: Axial curvature maps of the front corneal surface obtained with the Keratograph 5M (Oculus Optikgeräte GmbH, Wetzlar, Germany). We can observe a truncated bow tie and skewed radial axis pattern in OD, but innocent findings in OS. The bottom part of the figure presents Pentacam maps with Belin ABCD keratoconus staging

Clinical Examples

Forme fruste keratoconus

A 14-year-old young man with very asymmetric ectatic corneal disease who was referenced to our clinic for treatment, is presented in Fig. 3. Moderate keratoconus was noted in the left eye, which presented with uncorrected distance visual acuity of 20/50. The right eye had a relatively normal pattern, with very mild asymmetry and uncorrected distance visual acuity of 20/25. Manifest refraction was −0.50 −0.50 × 104 and +1.50 −4.75 × 169, giving 20/20 and 20/30–2 in OD and OS, respectively. Femtosecond laser-assisted intracorneal ring implant, associated with corneal CXL was proposed for the left eye, and the procedure was performed in February 2015. The Wavelight FS 200 was programmed to create a corneal tunnel at a 331 μm depth with an incision at 72°. The Keraring SI5 160°/250 micron (Mediphacos; Belo Horizonte, Brazil) corneal ring segment was chosen. Corneal CXL was performed using the fast mode with 18 mW/cm^2 for 5 min to provide a total energy of 5.4J (Avedro; Boston, USA). Fig. 4 demonstrates the effect of the combined intracorneal ring segment implantation with CXL, comparing pre (D) and pos operative (B) anterior corneal surface curvatures. At the bottom right part of the display we can also appreciate the anterior curvature post- and pre-operative difference map (B-D). Note the applanation effect, especially at the superior-temporal portion of the cornea.

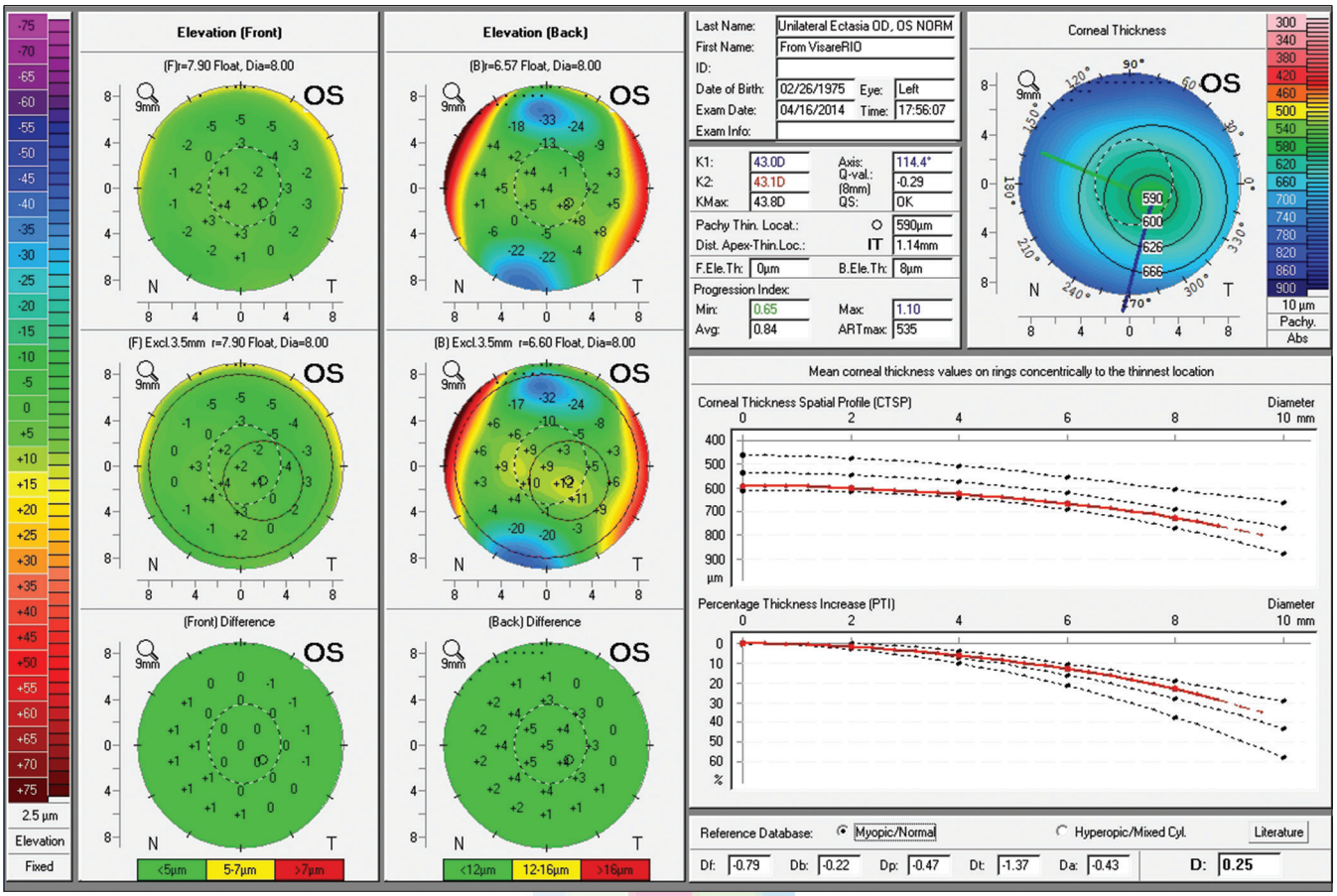

Figure 9: Belin-Ambrósio Enhanced Ectasia Display from the Pentacam of OS. Unremarkable findings are observed

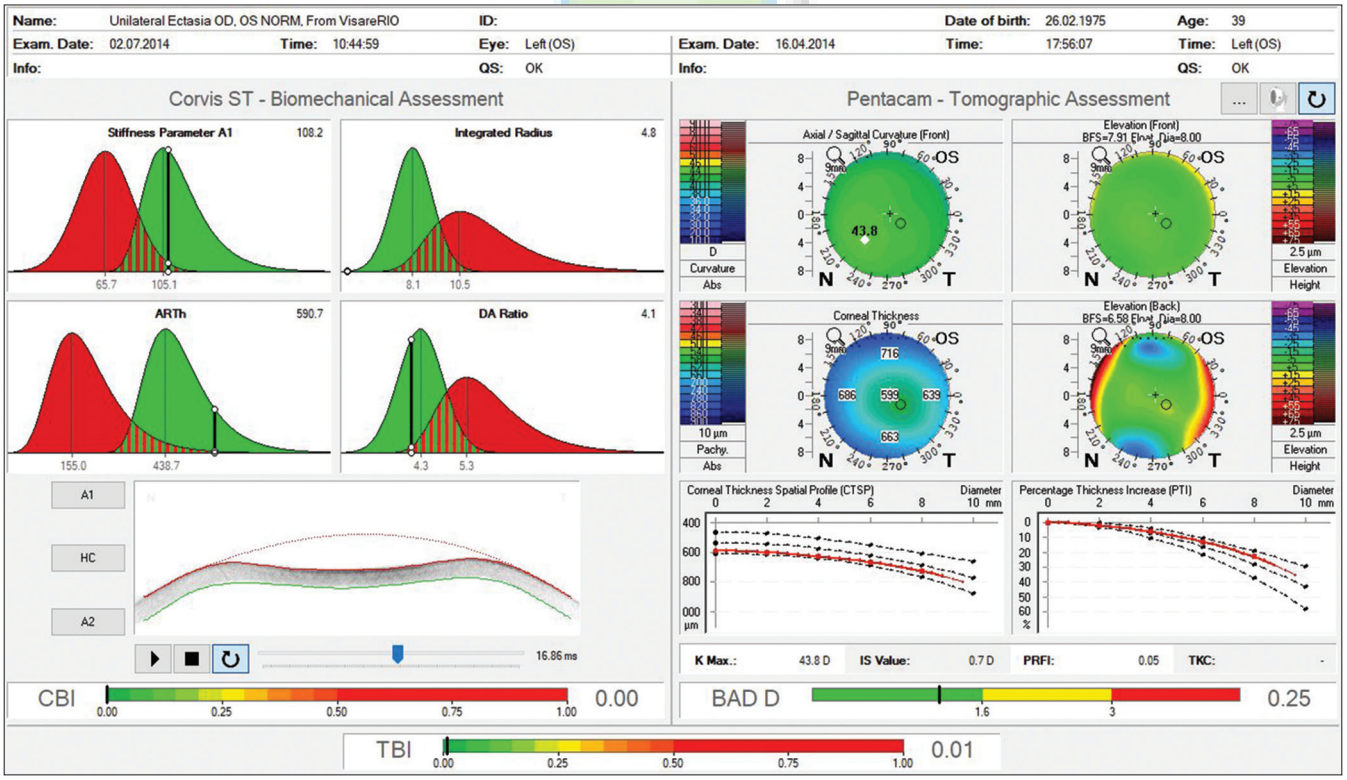

Figure 10: Pentacam/Corvis ST Ambrósio, Roberts and Vinciguerra tomographic/biomechanical index display

The fellow eye had a relatively normal Belin-Ambrósio Enhanced Ectasia Display (right eye) with no significant abnormalities in the elevation maps but relatively low ARTmax (Ambrósio's relational thickness to the maximal pachymetric progression meridian) of 371.[38] The BAD-D was 1.25 which is also considered relatively normal, along with corneal elevation data [Fig. 5].[16] Interestingly, the right eye showed nearly no curvature change during 2 years– Fig. 4a and c. In addition, the Belin ABCD progressions display [Fig. 6] was generated and did not show significant evolution since the first visit throughout the 2 years of documented follow-up.[39] Considering such longitudinal topometric and tomographical data, this case might have been considered to have unilateral keratoconus, as proposed in a recent article.[40] While we would rather refer to such cases as unilateral ectasia due to a secondary biomechanical event, considering the consensus that unilateral keratoconus does not exist,[12] advanced Scheimpflug analysis provides evidence of the enhanced sensitivity approach. The CBI from Corvis ST was 0.95 in the right eye [Fig. 7],[37] which is higher than 0.5 (threshold for detecting ectasia). Moreover, TBI was 0.74, which is higher than the cutoff range from 0.25 to 0.29 and thereby consistent with ectasia diagnosis in both eyes [Fig. 7]. We do not dispute the fact that unilateral ectasia might occur. Indeed, the latest keratoconus global consensus agrees that while keratoconus is a bilateral disease, but secondary ectasia might be induced by a purely mechanical process, and thus occurs unilaterally.[12] However, this case is an example that enhanced screening technologies, especially with the combination of different approaches, beyond corneal surface, might augment the ability to detect milder forms of the disease.

Unilateral ectasia

Fig. 8 presents the case of a 39 years-old male referred for specialized KC treatment. Manifest refraction was -1.75 -4.00 x 35 in OD and -0.50 -0.25 x 115 in OS, giving him 20/40 and 20/16 in OD and OS respectively. A marked irregularity with steep and truncated bow tie with skewed radial axis is noted in corneal topography from the right eye [Fig. 8a]. Front surface maps by Placido analysis were similar to corresponding Pentacam maps in both eyes. The Belin ABCD keratoconus staging was calculated and determined as A2B2C0D1 for OD and A0B0C0D0 for OS.[39] Elevation and pachymetric maps, along with pachymetric distribution graphs, were unremarkably normal in OS, with a BAD-D value of 0.25 [Fig. 9]. Fig. 10 illustrates the Pentacam/Corvis ST ARV (Ambrósio, Roberts and Vinciguerra) TBI display. CBI and TBI values are unremarkably normal in OS. Interestingly, this case was examined by very high-frequency digital ultrasound and Fourier-domain optical coherence tomography,[41] which demonstrated normal epithelial mapping patterns. The diagnosis of unilateral ectasia in this case was based on clinical findings, along with tomographic and biomechanical data.

Conclusion

Clinical evaluation of *in vivo* corneal biomechanics is a challenging, but promising area of contemporary ophthalmology. Understanding the biomechanical corneal deformation behavior might be useful in numerous clinical situations, including glaucoma and corneal ectatic diseases. The characterization of ectasia susceptibility goes beyond the detection of mild cases, which unquestionably enhances safety of elective refractive corneal LVC but also may improve its efficiency. While we can recognize significant improvements over the past years, additional research is still needed. Nevertheless, we anticipate an accelerated growth in knowledge in this field in the next years to come.

Declaration of patient consent

The authors certify that they have obtained all appropriate patient consent forms. In the form the patient(s) has/have given his/her/their consent for his/her/their images and other clinical information to be reported in the journal. The patients understand that their names and initials will not be published and due efforts will be made to conceal their identity, but anonymity cannot be guaranteed.

Financial support and sponsorship

Nil.

Conflicts of interest

Renato Ambrósio Jr., MD, PhD and Cynthia J. Roberts, PhD, are consults of OCULUS Optikgeräte GmbH. For the remaining authors none were declared.

References

1. Andreassen TT, Simonsen AH, Oxlund H. Biomechanical properties of keratoconus and normal corneas. Exp Eye Res 1980;31:435-41.
2. Liu J, Roberts CJ. Influence of corneal biomechanical properties on intraocular pressure measurement: Quantitative analysis. J Cataract Refract Surg 2005;31:146-55.
3. Dupps WJ Jr., Biomechanical modeling of corneal ectasia. J Refract Surg 2005;21:186-90.
4. Luce DA. Determining *in vivo* biomechanical properties of the cornea with an ocular response analyzer. J Cataract Refract Surg 2005;31:156-62.
5. Luz A, Faria-Correia F, Salomão MQ, Lopes BT, Ambrósio R Jr. Corneal biomechanics: Where are we? J Curr Ophthalmol 2016;28:97-8.
6. Roberts CJ, Dupps WJ Jr. Biomechanics of corneal ectasia and biomechanical treatments. J Cataract Refract Surg 2014;40:991-8.
7. Dupps WJ Jr., Roberts CJ. Corneal biomechanics: A decade later. J Cataract Refract Surg 2014;40:857.
8. Binder PS, Lindstrom RL, Stulting RD, Donnenfeld E, Wu H, McDonnell P, *et al*. Keratoconus and corneal ectasia after LASIK. J Cataract Refract Surg 2005;31:2035-8.
9. Ambrósio R Jr., Randleman JB. Screening for ectasia risk: What are we screening for and how should we screen for it? J Refract Surg 2013;29:230-2.
10. Ambrósio R Jr., Lopes BT, Faria-Correia F, Salomão MQ, Bühren J, Roberts CJ, *et al*. Integration of scheimpflug-based corneal tomography and biomechanical assessments for enhancing ectasia detection. J Refract Surg 2017;33:434-43.
11. McGhee CN, Kim BZ, Wilson PJ. Contemporary treatment paradigms in keratoconus. Cornea 2015;34 Suppl 10:S16-23.
12. Gomes JA, Tan D, Rapuano CJ, Belin MW, Ambrósio R Jr., Guell JL, *et al*. Global consensus on keratoconus and ectatic diseases. Cornea 2015;34:359-69.
13. Wilson SE, Ambrosio R. Computerized corneal topography and its importance to wavefront technology. Cornea 2001;20:441-54.
14. Maeda N, Klyce SD, Tano Y. Detection and classification of mild irregular astigmatism in patients with good visual acuity. Surv Ophthalmol 1998;43:53-8.
15. Ambrósio R Jr., Belin MW. Imaging of the cornea: Topography vs. Tomography. J Refract Surg 2010;26:847-9.

16. Ambrósio R Jr., Valbon BF, Faria-Correia F, Ramos I, Luz A. Scheimpflug imaging for laser refractive surgery. Curr Opin Ophthalmol 2013;24:310-20.
17. Smadja D, Touboul D, Cohen A, Doveh E, Santhiago MR, Mello GR, *et al.* Detection of subclinical keratoconus using an automated decision tree classification. Am J Ophthalmol 2013;156:237-460.
18. Ambrósio R Jr., Nogueira LP, Caldas DL, Fontes BM, Luz A, Cazal JO, *et al.* Evaluation of corneal shape and biomechanics before LASIK. Int Ophthalmol Clin 2011;51:11-38.
19. Ambrósio R Jr., Dawson DG, Salomão M, Guerra FP, Caiado AL, Belin MW, *et al.* Corneal ectasia after LASIK despite low preoperative risk: Tomographic and biomechanical findings in the unoperated, stable, fellow eye. J Refract Surg 2010;26:906-11.
20. Luz A, Lopes B, Hallahan KM, Valbon B, Ramos I, Faria-Correia F, *et al.* Enhanced combined tomography and biomechanics data for distinguishing forme fruste keratoconus. J Refract Surg 2016;32:479-94.
21. Tian L, Ko MW, Wang LK, Zhang JY, Li TJ, Huang YF, *et al.* Assessment of ocular biomechanics using dynamic ultra high-speed scheimpflug imaging in keratoconic and normal eyes. J Refract Surg 2014;30:785-91.
22. Ambrósio R Jr., Ramos I, Luz A, Faria-Correa F, Steinmueller A, Krug M, *et al.* Dynamic ultra high speed scheimpflug imaging for assessing corneal biomechanical properties. Rev Bras Oftalmol 2013;72:99-102.
23. Piñero DP, Alcón N. *In vivo* characterization of corneal biomechanics. J Cataract Refract Surg 2014;40:870-87.
24. Roberts CJ. Concepts and misconceptions in corneal biomechanics. J Cataract Refract Surg 2014;40:862-9.
25. Joda AA, Shervin MM, Kook D, Elsheikh A. Development and validation of a correction equation for corvis tonometry. Comput Methods Biomech Biomed Engin 2016;19:943-53.
26. Bao F, Deng M, Wang Q, Huang J, Yang J, Whitford C, *et al.* Evaluation of the relationship of corneal biomechanical metrics with physical intraocular pressure and central corneal thickness in *ex vivo* rabbit eye globes. Exp Eye Res 2015;137:11-7.
27. Bao F, Huang Z, Huang J, Wang J, Deng M, Li L, *et al.* Clinical evaluation of methods to correct intraocular pressure measurements by the goldmann applanation tonometer, ocular response analyzer, and corvis ST tonometer for the effects of corneal stiffness parameters. J Glaucoma 2016;25:510-9.
28. Faria-Correia F, Ramos I, Valbon B, Luz A, Roberts CJ, Ambrósio R Jr., *et al.* Scheimpflug-based tomography and biomechanical assessment in pressure-induced stromal keratopathy. J Refract Surg 2013;29:356-8.
29. Valbon BF, Ambrósio R Jr., Fontes BM, Alves MR. Effects of age on corneal deformation by non-contact tonometry integrated with an ultra-high-speed (UHS) scheimpflug camera. Arq Bras Oftalmol 2013;76:229-32.
30. Bak-Nielsen S, Pedersen IB, Ivarsen A, Hjortdal J. Repeatability, reproducibility, and age dependency of dynamic scheimpflug-based pneumotonometer and its correlation with a dynamic bidirectional pneumotonometry device. Cornea 2015;34:71-7.
31. Nemeth G, Hassan Z, Csutak A, Szalai E, Berta A, Modis L Jr., *et al.* Repeatability of ocular biomechanical data measurements with a scheimpflug-based noncontact device on normal corneas. J Refract Surg 2013;29:558-63.
32. Ali NQ, Patel DV, McGhee CN. Biomechanical responses of healthy and keratoconic corneas measured using a noncontact scheimpflug-based tonometer. Invest Ophthalmol Vis Sci 2014;55:3651-9.
33. Steinberg J, Katz T, Lücke K, Frings A, Druchkiv V, Linke SJ, *et al.* Screening for keratoconus with new dynamic biomechanical *in vivo* scheimpflug analyses. Cornea 2015;34:1404-12.
34. Salomão MQ, Faria-Correa F, Ramos I, Luz A, Ambrósio R Jr. Corneal deformation response with dynamic ultra-high-speed scheimpflug imaging for detecting ectatic corneas. Int J Keratoconus Ectatic Corneal Dis 2016;5:1-5.
35. Peña-García P, Peris-Martínez C, Abbouda A, Ruiz-Moreno JM. Detection of subclinical keratoconus through non-contact tonometry and the use of discriminant biomechanical functions. J Biomech 2016;49:353-63.
36. Lopes BT, Ramos I, Salomão MQ, Canedo AL, Ambrósio R Jr. Perfil paquimétrico horizontal para a detecção do ceratocone. Rev Bras Oftalmol 2015;74:382-5.
37. Vinciguerra R, Ambrósio R Jr., Elsheikh A, Roberts CJ, Lopes B, Morenghi E, *et al.* Detection of keratoconus with a new biomechanical index. J Refract Surg 2016;32:803-10.
38. Vinciguerra R, Ambrósio R Jr., Roberts CJ, Azzolini C, Vinciguerra P. Biomechanical characterization of subclinical keratoconus without topographic or tomographic abnormalities. J Refract Surg 2017;33:399-407.
39. Belin MW, Duncan JK. Keratoconus: The ABCD grading system. Klin Monbl Augenheilkd 2016;233:701-7.
40. Imbornoni LM, Padmanabhan P, Belin MW, Deepa M. Long-term tomographic evaluation of unilateral keratoconus. Cornea 2017;36:1316-24.
41. Ramos I, Reinstein DZ, Archer TJ, Gobbe M, Salomão MQ, Lopes B, *et al.* Unilateral ectasia characterized by advanced diagnostic Tests. Int J Keratoconus Ectatic Corneal Dis 2016;5:40-51.